ACS OMEGA

http://pubs.acs.org/journal/acsodf

Article

Preparation of Microfiltration Hollow Fiber Membranes from Cellulose Triacetate by Thermally Induced Phase Separation

Shota Takao, Saeid Rajabzadeh, Chihiro Otsubo, Toyozo Hamada, Noriaki Kato, Keizo Nakagawa, Takuji Shintani, Hideto Matsuyama, and Tomohisa Yoshioka*

Cite This: *ACS Omega* 2022, 7, 33783−33792

Read Online

ACCESS | Metrics & More | Article Recommendations | Supporting Information

ABSTRACT: For the first time, self-standing microfiltration (MF) hollow fiber membranes were prepared from cellulose triacetate (CTA) via the thermally induced phase separation (TIPS) method. The resultant membranes were compared with counterparts prepared from cellulose diacetate (CDA) and cellulose acetate propionate (CAP). Extensive solvent screening by considering the Hansen solubility parameters of the polymer and solvent, the polymer's solubility at high temperature, solidification of the polymer solution at low temperature, viscosity, and processability of the polymeric solution, is the most challenging issue for cellulose membrane preparation. Different phase separation mechanisms were identified for CTA, CDA, and CAP polymer solutions prepared using the screened solvents for membrane preparation. CTA solutions in binary organic solvents possessed the appropriate properties for membrane preparation via liquid−liquid phase separation, followed by a solid−liquid phase separation (polymer crystallization) mechanism. For the prepared CTA hollow fiber membranes, the maximum stress was 3−5 times higher than those of the CDA and CAP membranes. The temperature gap between the cloud point and crystallization onset in the polymer solution plays a crucial role in membrane formation. All of the CTA, CDA, and CAP membranes had a very porous bulk structure with a pore size of ∼100 nm or larger, as well as pores several hundred nanometers in size at the inner surface. Using an air gap distance of 0 mm, the appropriate organic solvents mixed in an optimized ratio, and a solvent for cellulose derivatives as the quench bath media, it was possible to obtain a CTA MF hollow fiber membrane with high pure water permeance and notably high rejection of 100 nm silica nanoparticles. It is expected that these membranes can play a great role in pharmaceutical separation.

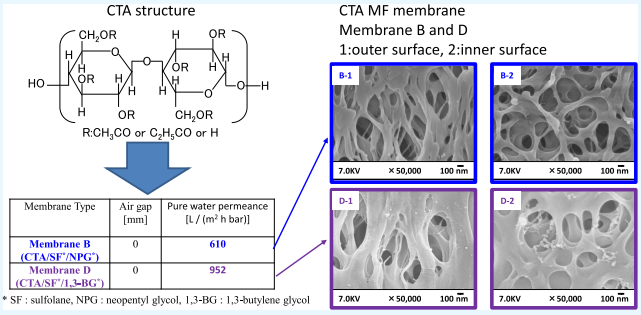

1. INTRODUCTION

The membrane separation process is considered one of the tentative approaches that potentially can help solve many global problems such as water shortage and greenhouse gas emissions and has attracted much attention over the last couple of decades. In addition to treating water (including wastewater) and gas separation and purification, membrane separation technology has also been applied to blood plasma separation and the purification and concentration of industrial products. Although poly(vinylidene fluoride) (PVDF) and polyethersulfone (PES) are the most common membrane materials, they experience considerable fouling, especially in medical applications, because of their hydrophobic nature and low hemocompatibility.[1] Membranes prepared from cellulose-based materials possess considerable hemocompatibility.[2] However, intermolecular hydrogen bonding in natural cellulose causes poor processability, and it is difficult to melt or dissolve these materials to fabricate membranes.[3] Rather, soluble derivatives of cellulose such as cellulose acetate (CA), cellulose diacetate (CDA), and cellulose triacetate (CTA) are preferred materials for membrane preparation.[2,4−6]

Leob-Sourirajan first used CA to prepare reverse osmosis (RO) membranes in the 1960s, and subsequently, different cellulose derivatives were widely used to prepare RO, forward osmosis (FO), and dialysis membranes.[1,2,4−8] Among these cellulose derivatives, CTA has several advantages over others including higher hemocompatibility, lower fouling tendency, better resistance against chemicals and biodegradation, improved mechanical strength, better temperature tolerance, and lower cost.[9,10] Therefore, CTA is a favorable material for membranes, although its processing is relatively more complicated due to the low solubility in solvents.[11]

CDA microfiltration (MF) membranes have been widely used in pharmaceutical separation and purification, and they displayed considerable fouling resistance.[4,8,12−14] However,

Received: March 23, 2022
Accepted: August 31, 2022
Published: September 16, 2022

when the CDA membrane is used in a culture solution, it is degraded by the microorganisms therein.[15,16] Because CTA has a relatively higher resistance to degradation than other cellulose derivatives, the related membranes are more stable.[17]

A large amount of cellulose derivative membranes are prepared by non-solvent-induced phase separation (NIPS). Most of these membranes have a dense surface structure for RO, FO, and dialysis applications. Some researchers also prepared ultrafiltration (UF) membranes from CTA via the NIPS method.[2,5−8] As an alternative to the NIPS method, the thermally induced phase separation (TIPS) method can use a much wider variety of solvents to dissolve the polymer, allows easier control of membrane preparation, and produces a much more porous structure than the NIPS membrane and a narrower pore size distribution.[18−20] Despite these promising characteristics, a few studies have applied TIPS to prepare cellulose-based membranes.

Shibutani et al.[21] prepared hollow fiber membranes using different CA derivatives via the TIPS method and obtained UF membranes with dense outer surface structures. They compared fouling on membranes prepared from CDA, acetate butyrate (CAB), and cellulose acetate propionate (CAP). The prepared membranes exhibited pure water permeances of 316, 406, and 355 L/(m^2·h·bar) for CDA, CAB, and CAP, respectively. With its highest hydrophilicity, CDA showed the least fouling in BSA (bovine serum albumin) and humic acid solutions and the highest recovery after backwashing among all prepared membranes. Fu et al.[22] used CAB to prepare hollow fiber membranes using NIPS and TIPS methods. They evaluated the effects of the air gap, bath temperature, and composition on the outer surface structure of the membrane. A dense surface was obtained in most cases using either NIPS or TIPS, while hollow fiber membranes with a porous structure were obtained using a high solvent composition in a coagulation bath at zero air gap and high bath temperature.

Yu et al.[11] prepared novel flat-sheet CTA membranes using the TIPS method, with dimethyl sulfone ($DMSO_2$) as the solvent and poly(ethene glycol) (PEG400) as the crystallizable solvent and additive. The resultant membranes featured a cellular structure suitable as a substrate for thin-film composite FO membranes. The top and bottom surfaces of the membranes were very dense, except when the researchers used a very low polymer concentration (5 wt %), high bath temperature, and optimal solvent and additive composition in the polymeric solution. The water permeance was less than 150 L/(m^2·h·bar) even in the case of a soft and ductile membrane with 5 wt % CTA. In another study,[23] Xing et al. prepared CTA flat-sheet UF membranes using N-TIPS, which combines the NIPS and TIPS methods. Although their approach produced a very porous bottom surface with a pore size of ∼1 μm, the structure on the outer surface was still dense. Similar to the previous study, a low polymer concentration (8 wt %), a high bath temperature, and a high solvent content in the bath were used to obtain a porous membrane with a pore size of ∼50 nm. Notably, it is very difficult or impossible to obtain hollow fiber membranes using the approach described in the previous studies[11,23] mainly because of the low polymer concentration in the solution.

Considering the fascinating antifouling properties, biocompatibility, and resistance against biodegradation, there is a significant demand for CTA-based MF membranes in biological and pharmaceutical applications. There have been considerable studies on preparing cellulose derivative membranes, but most of them focused on dense membranes made mainly using CDA and CAP, while porous CTA membranes were rarely reported. An extensive and comprehensive search of the literature revealed only two reports on fabricating CTA MF flat-sheet membranes.[11,23] Further, the conditions used in those studies were very challenging (e.g., very low polymer concentrations <8 wt %, special bath composition, and high bath temperature), which resulted in extremely low mechanical strengths. Especially, the preparation of a self-standing CTA MF hollow fiber membrane has not been reported.

For the first time, here, we prepared a self-standing CTA MF hollow fiber membrane after the comprehensive solvent screening. Using a mixture of two selected solvents, we produced a membrane with high pure water permeance (PWP) of ∼1000 L/(m^2·h·bar) and almost complete rejection of 100 nm silica nanoparticles. The temperature gap between the cloud point and crystallization onset of the polymer solution plays a crucial role in membrane formation. The results were compared with those of CDA and CAP hollow fiber membranes. The use of a zero air gap distance and a solvent as the quench bath media was the key to obtain high PWP and considerable nanoparticle rejection in the CTA MF hollow fiber membrane.

2. EXPERIMENTAL SECTION

2.1. Materials. Figure 1 shows the chemical structures of cellulose derivatives used in this study, and Table 1 lists the polymer properties. Three cellulose derivatives were used: cellulose triacetate (CTA; manufactured by Daicel, Japan, MW = 405 000), cellulose diacetate (CDA; manufactured by Daicel, Japan, MW = 219 000), and cellulose acetate propionate (CAP; manufactured by Eastman, MW = 189 000). As shown in Table S1, 61 solvents were selected with a boiling point of 180 °C or higher and a Hanssen solubility parameter (HSP) in the range of 18−34 [J/cm^3]$^{0.5}$. This HSP range was chosen due to its suitability for the TIPS method. Specifically, the HSP values of the polymer (21.6−23.0 [J/cm^3]$^{0.5}$, Table S1) and the solvent should be neither very close (NIPS solvent) nor

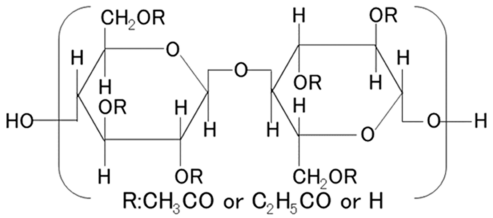

Figure 1. Chemical structure of the cellulose derivatives. Three derivatives were used in this study with different R groups (which are listed in Table 1).

Table 1. Polymer Properties

			substitution ratio[a]	
polymer	melting point (T_m, °C)	MW	R:CH_3CO	R:C_2H_5CO
CTA	300	405 000	2.87	
CDA	235	219 000	2.44	
CAP	191	189 000	0.07	2.58

[a]Ratio of the esterified groups of three hydroxy groups per glucose unit.

https://doi.org/10.1021/acsomega.2c01773
ACS Omega 2022, 7, 33783−33792

very far from each other (nonsoluble solvent for polymer). The main solvents we used were 2-ethyl-1,3-hexanediol (EHD; Wako Pure Chemical Industries, Ltd., Japan, ≥98.0%), sulfolane (SF; Wako Pure Chemical Industries, Ltd., Japan, ≥95.0%), 1,3-butylene glycol (1,3-BG; Wako Pure Chemical Industries, Ltd., Japan, special grade, ≥98.0%), and neopentyl glycol (NPG; Tokyo Chemical Industry, Japan, >98.0%). Ethanol (Wako Pure Chemical Industries, Ltd., Japan, special grade, ≥99.5%) was used to extract the organic solvent remaining in the structure of the prepared membrane.

2.2. Solvent Screening. HSP is the first criterion in screening the potential solvents to ensure a suitable polymer solubility to form a homogeneous polymeric solution for membrane fabrication. The HSP of a chemical (δ_t [(J/cm^3)$^{0.5}$]) is contributed by three types of interactions: dispersion (δ_d), dipole interaction (δ_p), and hydrogen bonding (δ_h), according to eq 1

$$\mathrm{HSP} = \delta_t = (\delta_d^2 + \delta_p^2 + \delta_h^2)^{0.5} \quad (1)$$

The affinity between the polymer (subscript 1) and solvent (subscript 2) can be determined from the difference in their HSP values, which is denoted by R_a and expressed by eq 2[24]

$$R_a = (4(\delta_{d1} - \delta_{d2})^2 + (\delta_{p1} - \delta_{p2})^2 + (\delta_{h1} - \delta_{h2})^2)^{0.5} \quad (2)$$

A smaller R_a value indicates a higher affinity between the polymer and the solvent. Generally, solvents appropriate for the TIPS process are capable of dissolving the polymer at high temperatures but only do so poorly at room temperature. Therefore, for a good candidate solvent in TIPS, the R_a value (the difference in HSP between the polymer and solvent) should be neither too small nor too large so that the solvent can dissolve the polymer, undergo phase separation, and form porous structures. Table S1 shows the HSP values between the cellulose derivative polymers and 61 solvents considered in solvent screening.

In the solvent screening test, the polymer (0.3, 0.4, and 0.5 g) and solvent (1.7, 1.6, and 1.5 g) were weighed and put into a test tube to prepare polymer solutions at the concentrations of 15, 20, and 25 wt %, respectively. The mixture was heated on an aluminum block at 170 °C and stirred for 3 h to obtain a homogeneous and transparent polymeric solution. Afterward, the test tube was placed in a holder and cooled to room temperature in the air. At this point, we checked whether the dope in the test tube became a white solid or not. The first criterion used for solvent screening is that the system should appear as a homogeneous polymeric solution at 170 °C and solidifies at room temperature. Table S2 shows the R_a values of polymers and solvents that satisfy this criterion. The second criterion for solvent screening is that the polymeric solution should have an appropriate (i.e., not very low) viscosity at a high temperature, which was judged by visual observation. Meanwhile, the manual tactile examination was made to ensure that the solution solidifies well at room temperature to produce a solid polymer with good mechanical strength. These material characteristics are considered suitable for the TIPS process. Table S3 shows the R_a values of the polymers and solvents that satisfy the second screening criterion. As will be described below, the solvents we identified as suitable for the TIPS method were: EHD for CDA and CAP membranes; NPG, 1,3-BG, and SF for CTA membranes. According to Tables S4 and S5, these polymers and solvents have an intermediate difference in their HSP values, namely, neither very small nor large.

2.3. Phase Separation Temperature Measurement. After the solvent screening (Table S2), ∼6 to 8 mg of polymer solution in the identified solvent was weighed and sealed in an aluminum pan. The pan was inserted into a differential scanning calorimeter (DSC Q8000, TA Instruments) to measure the crystallization temperature of the solutions under a nitrogen atmosphere. The same instrument was also used to measure the melting temperatures of the pure polymers CTA, CDA, and CAP. The pan was heated from room temperature to 190 °C, held for 2 min, and then cooled to 0 °C at a rate of 10 °C/min.

A piece of the solidified polymer solution was sandwiched between two pieces of the cover glass to measure the cloud point. A Teflon sheet with a thickness of 100 μm was used to seal the sample between the cover glass, maintaining the appropriate spacing while preventing evaporation during heating. The sample was placed on a hot stage (Linkam, HFS91, U.K.), heated from room temperature to 190 °C, held for 1 min, and then cooled to 25 °C at a rate of 10 °C/min. The cloud point was observed visually by noting the appearance of turbidity under an optical microscope (Olympus BX50, Japan).

2.4. Preparation of Hollow Fiber Membrane. Three cellulose derivatives (CTA, CDA, and CAP) were used to prepare hollow fiber membranes. EHD was used as the solvent for CDA and CAP, and two mixtures of NPG/SF and SF/1,3-BG were used for CTA. The compositions of the mixtures are given in Table 2. The selection process of the solvents will be further described in Section 3.1.

Figure 2 shows a schematic of the apparatus (BA-0, Imoto Co., Japan) used to fabricate the hollow fiber membranes via

Table 2. Preparation Conditions of Hollow Fiber Membranes Based on Cellulose Derivatives

preparation conditions		parameters
polymer solution composition (wt %)	CTA/SF/NPG (membrane A, B)	20/16/64
	CTA/SF/1,3-BG (membrane C, D)	20/16/64
	CDA/EHD (membrane E)	20/80
	CAP/EHD (membrane F)	20/80
air gap (mm)		5 mm air gap for membranes A, C, E, and F
		0 mm air gap for membranes B and D
polymer dissolution time (h)		6
spinning temperature (°C)		160 °C for CTA membrane
		180 °C for CDA membrane
		140 °C for CAP membranes
polymer solution flow rate (g/min)		15−25
bore liquid		1,3-BG for CTA membrfane and EHD for CDA and CAP membranes
bore liquid flow rate (g/min)		5.76
quenching bath liquid		1,3-BG for CDA and CTA membranes and water for CAP membrane
quenching bath temperature (°C)		room temperature
take-up speed (m/min)		24

https://doi.org/10.1021/acsomega.2c01773
ACS Omega 2022, 7, 33783−33792

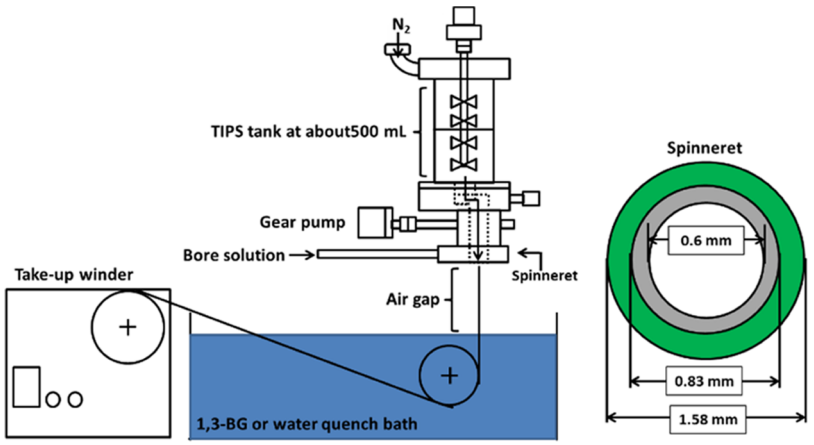

Figure 2. Schematic diagram of the apparatus used to fabricate hollow fiber membranes via the TIPS process.

the TIPS process. In brief, predetermined amounts of polymer (CTA, CDA, or CAP) and solvent (SF/NPG, SF/1,3-BG, or EHD) were fed to the mixing tank and mixed with stirring blades at 180 °C for 6 h to obtain a homogeneous polymer solution. Then, the system was set to a predetermined temperature (shown in Table 2) that was several tens of degrees higher than the cloud point to ensure an appropriate solution viscosity for spinning. After holding this temperature for 1 h to release air bubbles, the polymer solution was fed to a spinneret by a gear pump under pressured nitrogen of 0.04−0.1 MPa. Simultaneously, the bore liquid was sent to the spinneret using a peristaltic pump (Perista pump, SJ-1211, ATTO Corporation, Japan). The spinneret consisted of outer and inner channels with respective diameters of 1.58 and 0.83 mm. The bore liquid was introduced into the internal orifice to create a lumen within the hollow fibers. The hollow fiber membrane was extruded from the spinneret and wound on a take-up winder, after entering a quench bath to induce phase separation and solidify the membrane. 1,3-BG was used as the quench bath for CTA and CDA, whereas water was used for CAP. Since the HSP of the 1,3-BG is much closer to the used solvents rather than that of the water, using 1,3-BG resulted in a more porous outer surface.[25,26] Thus, when 1,3-BG was used as the quenching medium, the membrane surface porosity became controllable. However, this bath could not be used to prepare CAP hollow fiber membranes because the polymer solidified at an extremely slow rate. Thus, water was used as the quenching liquid instead of for the CAP membrane.

This study aimed to prepare the MF CTA membrane with as large as possible surface and porous bulk pore size. In this regard, decreasing polymer concentration is the most straightforward approach. However, it should be kept in mind that for preparing a hollow fiber membrane, self-standing membrane, since there is no backing fabric, the polymeric solution and membrane strength should reach an adequate value to be practically possible to prepare a membrane and use as a hollow fiber membrane. Although not shown here, we noted that when the polymer concentration decreases to less than 20 wt %, the hollow fiber membrane preparation condition is practically challenging and unstable because of the low viscosity of the polymeric solution. In reality, it was difficult to obtain hollow fiber membranes. Thus, a polymer concentration of 20 wt % as the minimum possible concentration to get the MF hollow fiber membrane was selected for this study. After solvent screening tries and error, we discover that polymer concentration around 20 wt % is optimal for getting MF membrane with stable and easy membrane preparation. Thus, in this study, the polymer concentration was fixed at 20 wt % (the minimum possible value) to obtain a hollow fiber membrane with high porosity. We also varied the air gap distance (see Figure 2) used in preparing CTA hollow fiber membranes from 5 to 0 mm to evaluate its effect and obtain membranes with high water permeance. The CAP and CDA membranes were prepared for comparison. Unfortunately, all our efforts to prepare CDA and CAP membranes with 0 mm air gap distance were unsuccessful, and membrane preparation was technically impossible. Thus, the air gap distance in those cases was fixed at 5 mm. It is very well evaluated and reported in the literature that using a shorter air gap distance resulted in the decreasing evaporation amount of the hot solvent from the outer surface of the extruded polymeric solution during the air gap distance, more porous structure forms at the outer surface of the membrane, larger and more pores appear at the outer surface of the membrane. Subsequently, the pure water permeability of the membrane increases by decreasing the air gap distance. That is why, we tried to keep the air gap as low as possible, zero in this study, in case it is practically possible in this study.[27−30]

2.5. Evaluation of the Prepared Hollow Fiber Membranes. *2.5.1. SEM Observation.* Immediately after membrane fabrication, the residual solvent in the bulk was exchanged by immersing the membrane sequentially in ethanol, diethyl ether, and hexane for 30 min, respectively. Membranes prepared using NPG and SF as solvent were immersed in ethanol for 2 weeks to ensure complete solvent extraction, considering the high melting points of these chemicals (129 and 27.5 °C, respectively). Subsequently, the membranes were air-dried for 1 h and then kept overnight in a dryer at 55 °C. After fracturing the dry hollow fiber membranes in liquid nitrogen and sputtering with Pt, the cross section, outer surface, and inner surface of membranes were observed using field emission scanning electron microscopy (FE-SEM, JEOL, JSF-7500F, Tokyo, Japan) at a scanning voltage of 3.0 kV.

2.5.2. Water Permeance. To evaluate the pure water permeance (PWP) through such a membrane, the sample was first immersed in ethanol for 2 weeks and then washed with running water for 30 min. PWP was measured using a method similar to that described in our previous work.[25] Pure water

https://doi.org/10.1021/acsomega.2c01773
ACS Omega 2022, 7, 33783−33792

was forced to permeate from the inside to the outside of the hollow fiber membrane at a transmembrane pressure of 0.1 MPa. This inside-out permeation test was used due to its ease of operation. The pure water permeance, J_w (L/(m^2·h·bar)), was calculated by eq 3 on the basis of the inner surface area of the hollow fiber membrane, volume of the permeated water, and time.

$$J_w = \frac{V}{At} \tag{3}$$

where V is the permeation volume of pure water (L), A is the inner surface area of the membrane (m^2), and t is the permeation time (h). The water permeability was measured for several specimens of the prepared membranes, and only average values are reported.

2.5.3. Particle Rejection. The particle rejection experiment was performed by flowing a feed solution of nanoparticles through the outer surface of the membrane (the dense layer). Water permeated from the outer surface to the inner surface, as described in our previous work.[22] The feed solution consisted of silica particles (100 nm, Quarton@, PL-7 grade, Fuso Chemical Industry, Japan) at 100 ppm suspended in pure water. Particle concentrations in the filtrate and feed solution were measured using a portable turbidity meter (HACH 2100P, Hach Co., Tokyo, Japan) with visible light in the 400−600 nm wavelength range. The particle rejection R is defined using eq 4

$$R = 1 - \left(\frac{C_f}{C_0}\right) \tag{4}$$

where C_0 and C_f are particle concentrations in the feed and permeate, respectively.

2.5.4. Mechanical Strength. The maximum stress at break and elongation of the hollow fiber membranes were measured using a tensile testing instrument (EZ-SX, Shimadzu Co.Japan). Membranes were fixed vertically between two pairs of tweezers with a length of 50 mm and then extended at a constant elongation rate of 20 mm/min until failure.

All experiments in this study were repeated at least three times, and the maximum standard deviation was less than 8% all over the results.

3. RESULTS AND DISCUSSION

3.1. Solvent Screening for Membrane Preparation Via TIPS. Two-step screening was carried out to select the appropriate solvents for preparing cellulose derivative hollow fiber membranes based on CTA, CDA, and CAP polymers. As explained in Section 2.2, the first criterion is that the R_a value (the distance in HSP between the polymer and solvent) falls within a predetermined range and that the polymer has good solubility in the solvent at a high temperature (170 °C). The second screening criterion according to Section 2.2 concerns the viscosity and solidification of the polymeric solution, as well as the mechanical strength of the solidified polymer solution based only on optical observation. The results are summarized in Table S4.

Only 10 of the considered solvents could dissolve CTA, and they fall within the range of R_a = 3.4−12.7 [(J/cm^3)$^{0.5}$], while the number of solvents appropriate for the dissolution of CDA and CAP is 37 (R_a = 2.8−12.8 [(J/cm^3)$^{0.5}$]) and 51 (R_a = 1.7−13.3 [(J/cm^3)$^{0.5}$]), respectively. These results are presented in Table S2, and their trends are consistent with the melting point of pure polymers measured using DSC in this study. Because CTA has a higher melting point (300 °C) than CDA (235 °C) and CAP (191 °C), fewer solvents are expected to dissolve CTA even at high temperatures. After considering the processability of selected solvents (the second criterion of screening), only one solvent was found suitable for CTA (NPG, R_a = 5.3 [(J/cm^3)$^{0.5}$]), 16 solvents were found for CDA with R_a = 2.3−8.9 [(J/cm^3)$^{0.5}$], and 20 solvents for CAP with R_a = 2.4−10.7 [(J/cm^3)$^{0.5}$]. These results are shown in Table S3.

Finally, we selected EHD as the solvent for preparing the CDA and CAP hollow fiber membranes based on the HSP evaluation, acceptable viscosity, solidification of polymer solutions at room temperature, good mechanical strength after solidification (processability to prepare hollow fiber membrane), and our previous experience.[32] The prepared CAP and CDA membranes were used for performance comparison with the CTA membrane. R_a values for the polymers and selected solvents are summarized in Tables S4 and S5.

Although NPG passed all screening criteria as an appropriate TIPS solvent for CTA, it was impossible to prepare a CTA membrane using NPG as a solvent in a simple polymer and diluent system because this polymeric solution system showed a low viscosity and solidification rate in the quench bath during hollow fiber membrane preparation. Based on our evaluation in the solvent screening section, we noted that using SF improves the CTA and NPG polymeric solution processability (viscosity and solidification rate). Thus, a mix of two solvents (NPG and SF) was used. It is inevitable to mention that although CTA/SF polymeric solution system makes a completely homogeneous solution with nice processability at high temperatures, by cooling down, this polymeric solution undergoes gelation at low temperatures. Thus practically, SF can be considered an additive to improve the processability of the polymeric solution to make a self-standing hollow fiber membrane. It should be emphasized that the polymeric solution-phase separation mechanism should not change to gelation that is not appropriate for membrane preparation. As shown in Table S6, SF/NPG ratio was optimized, and among different ratios, 1/4 showed the optimum solvents ratio with no gelation during colling polymeric solution and appropriate CTA polymeric solution processability to prepare self-standing hollow fiber membrane with appropriate polymeric solution viscosity.

We eventually used two binary solvents (SF/NPG and SF/1,3-BG, Table 2) to prepare the corresponding hollow fiber membranes for the following reasons.

Based on our extensive experimental and technical experience, we found that adding SF to the CTA/NPG solution improved the processability, and the spun CTA hollow fiber membrane became more accessible and stable. Thus, SF was used as an additive to improve the processability and the spinning stability. It is worth mentioning that our solvent screening test showed that the CTA/SF solution became a gel at room temperature, which is not suitable for preparing hollow fiber membranes at all. We add NPG with a high melting point to avoid gelation of CTA/SF in the membrane. We change the SF/NPG ratio as in Table S6. From the SF/NPG of 1 to 1/3, still gelation happens in CTA/SF/NPG system. When the SF/NPG ratio reached 1/4, no gelation was observed. It is worth mentioning that for SF/NPG of 1/5, gelation was not observed, but the cloud point increased sharply. It means the membrane preparation

https://doi.org/10.1021/acsomega.2c01773
ACS Omega 2022, 7, 33783−33792

temperature should be at a higher temperature and subsequently solution viscosity decrease. This decreasing solution viscosity makes membrane preparation a challenge. That is the reason we used SF/NPG with a 1/4 ratio for this study.

As will be discussed in the following sections of the manuscript. The prepared membranes from the CTA/SF/NPG system showed not much interesting results in terms of membrane performance. Alternatively, another polymeric system using SF and 1,3-BG mixture was used to make the membrane. Again similar to the CTA/SF/NPG system there is an optimal ratio for SF/1,3-BG. Here in this system, SF plays the key role of the solvent. However, as mentioned above, CTA/SF undergoes gelation at low temperatures. Thus, 1,3-BG as a nonsolvent was added to induce phase separation before the happing of the gelation at low temperature. The reason why we focused on 1,3-BG among the many nonsolvents of CTA is that 1,3-BG is a green solvent and is used in cosmetics. Many ratios of SF/1,3-BG were evaluated in the solvent screening step to see the thermodynamic and processability of the mixture solution to prepare the membrane. When the polymeric solution is made with a high content of SF, a low amount of 1,3-BG gelation happens. On the contrary, a polymeric solution with a very high amount of 1,3-BG and a low content of SF is not able to make a homogeneous solution or comes with an extremely high cloud point that makes membrane preparation impossible practically. Thus, there is an optimum amount between these two extremes (high content of SF with gelation polymeric solution, and high content of 1,3-BG with solubility problem). Many ratios of SF/1,3-BG were evaluated in the solvent screening step to see the thermodynamic and processability of the mixture solution to prepare membrane. After varying the SF/1,3-BG ratios, the mixture of SF and 1,3-BG was found more suitable with the optimum weight ratio of 1:4, which showed a polymer mixture with appropriate cloud point and stable membrane spinning conditions, as well as desirable solidification rather than gelation after quenching. As will be described below, a polymer solution of CTA in SF/1,3-BG with the composition in Table 2 resulted in an excellent MF membrane structure with a high water permeance performance.

3.2. Phase Diagram of Cellulose Derivatives for the TIPS Method. Figure 3 shows the phase separation temperatures of cellulose derivatives in the solvents identified by screening. Only a cloud point was observed in the CDA/EHD solution, which is in line with our previous reports[21,32] and the results of other researchers.[33,34] Both a cloud point and a subsequent crystallization temperature were observed for the other two polymer solutions (CAP/EHD and CTA/NPG). In both polymer solutions, the cloud point was near the crystallization temperature with a gap of less than 17 °C. The cloud points were in the order CDA > CTA > CAP. The crystallization temperature was ∼109 °C for CTA/NPG and 67 °C for CAP/EHD. The crystallization temperature of CTA/NPG was higher than that of CAP/EHD because of its higher melting point. It is imperative to keep in mind that, although both CAP/EHD and CTA/NPG undergo liquid−liquid phase separation (as indicated by the cloud point), their subsequent crystallization is entirely different. We believe that CAP/EHD undergoes solid−liquid phase separation during crystallization, while CTA/NPG undergoes a mixed process of polymer crystallization and solvent crystallization because the

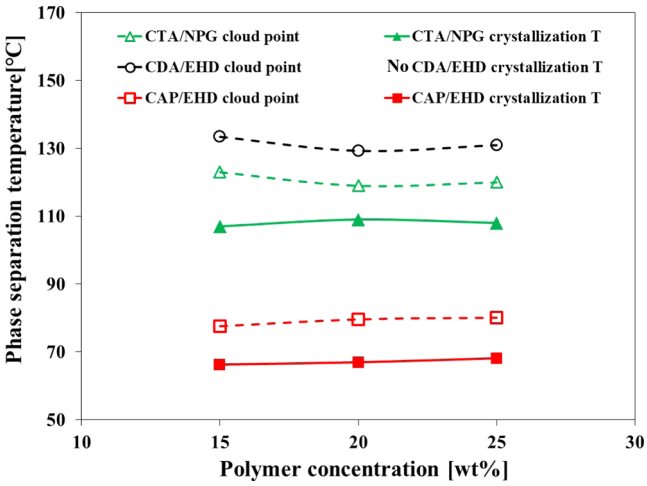

Figure 3. Phase diagram of cellulose derivative solutions. Filled symbols with solid lines: crystallization temperatures; empty symbols with dashed lines: cloud points; black circles: CDA/EHD solution; green triangles: CTA/NPG solution; and red squares: CAP/EHD solution. CDA/EHD did not display a cloud point; hence, the corresponding data are absent.

melting point of NPG (129.1 °C) is higher than the crystallization temperature observed for the CTA/NPG system (∼109 °C). The DSC thermogram cooling curve (not shown) from 180 to 30 °C displayed only one peak at ∼109 °C, which is attributed to the crystallization of the CTA polymer. At lower temperatures, there was another peak at around 27 °C due to the freezing of NPG. Similar phenomena were observed by Yu et al.[11] and Xing et al.[23] in the CTA/DMSO2/PEG400 polymer solution. Although the freezing point of $DMSO_2$ is 109 °C, only one crystallization peak was observed at around 45−50 °C in their studies. Thus, the solidification mechanisms of CTA/NPG and CAP/EHD are entirely different.

As explained in Section 3.1, it can be difficult to prepare CTA membranes using a single solvent, and a ternary polymer solution containing two solvents was used. The ratio of the two solvents should also be optimized. Hence, we investigated the phase diagrams of ternary systems consisting of CTA and two solvents (SF/1,3-BG and SF/NPG). Figure 4 shows the phase diagrams of the two systems. The cloud point was ∼140 °C for CTA/SF/1,3-BG and 100 °C for CTA/SF/NPG, and the respective crystallization temperatures were ∼91 and 80 °C.

It is clear from Figure 4 that CTA/SF/1,3-BG has a wider binodal region (from the cloud point to the crystallization temperature) than CTA/SF/NPG. Therefore, during phase separation, the time interval from the onset of liquid−liquid phase separation to polymer crystallization is longer for the CTA/SF/1,3-BG system. This results in a longer coarsening time for the droplets generated by liquid−liquid phase separation and larger pores in the prepared membrane structure.[20,35,36] A comparison of Figures 3 and 4 shows that the time interval between the onset of liquid−liquid phase separation and polymer crystallization for the mixed solvent is much longer than that for single-solvent systems. In particular, this time interval is very long for the CTA/SF/1,3-BG system. Thus, the CTA/SF/1,3-BG system is more suitable for forming membranes with superior structures and better performances, which we will prove in subsequent sections.

3.3. Membrane Structure and Performance. *3.3.1. Membrane Structure.* Structures of membranes

https://doi.org/10.1021/acsomega.2c01773
ACS Omega 2022, 7, 33783−33792

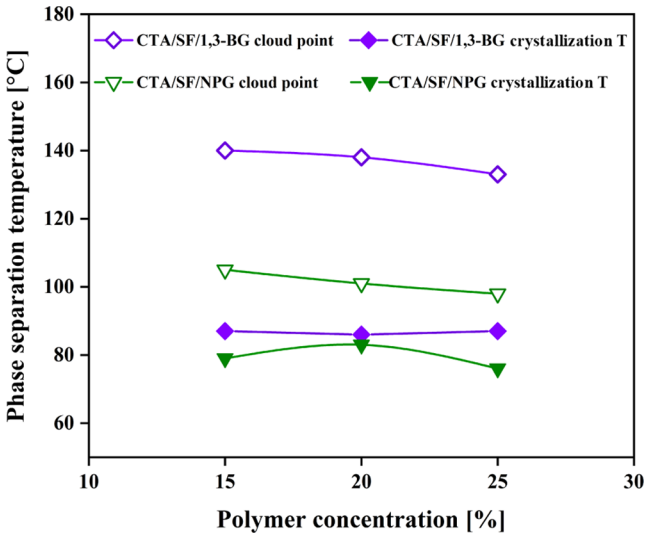

Figure 4. Phase diagram of CTA solutions in two mixed organic solvent systems. Filled symbols: crystallization temperature; empty symbols: cloud point; purple diamonds: CTA/SF/1,3-BG; green triangles: CTA/SF/NPG. The ratios were SF/NPG = SF/1,3-BG = 1/4 w/w.

prepared from different cellulose derivatives were evaluated using FE-SEM, and the results are summarized in Figures 5 and 6. Figure 5 shows the cross sections near the outer surface ("1", left column) and near the inner surface ("2", right column). Overall, we saw no significant difference among the membranes A–F, all of which showed a completely porous interconnected structure with a pore size of ~100 nm or larger rather than the spherical structure seen in many other studies.[6,11,18,21−23,31−35,37,38] From Figures 3 and 4, the cloud point is higher than the crystallization temperature in all systems. Therefore, interconnected structures were formed here due to the liquid phase separation. Considering the cross-sectional structures near the inner and outer surfaces of all membranes (A–F), the structure was completely porous with a pore size of ~100 nm or larger, which is what we expected when using a relatively low polymer concentration of 20 wt %. In Figure 5, the pore sizes of membranes A and B near the outer surface (images A-1 and B-1) appear to be slightly smaller than those of membranes C and D near the outer surface (C-1 and D-1). As explained by the phase diagram (Figure 4), the time interval from the onset of liquid–liquid phase separation (cloud point) to crystallization and the duration of the subsequently coarsening process were longer for membranes C and D (the CTA/SF/1,3-BG) than those for membranes A and B (CTA/SF/NPG). This is why, C and D showed slightly larger pores on their cross sections near the outer surface than those of A and B.

Although membranes A–F all displayed very similar cross-sectional structures in Figure 5, Figure 6 reveals that their inner and outer surface structures are completely different. Regardless of the type of cellulose derivative, membranes prepared using a 5 mm air gap distance had a dense surface or only contained a few tiny surface pores (<10 nm) because the larger air gap distance facilitates solvent evaporation from the outer surface of the membrane (Figure 6A-1,C-1,E-1,F-1).[20,36,39] In contrast, Figure 6B-1,D-1 (CTA membranes with different solvent compositions and 0 mm air gap distance) shows completely porous outer surfaces with large pores

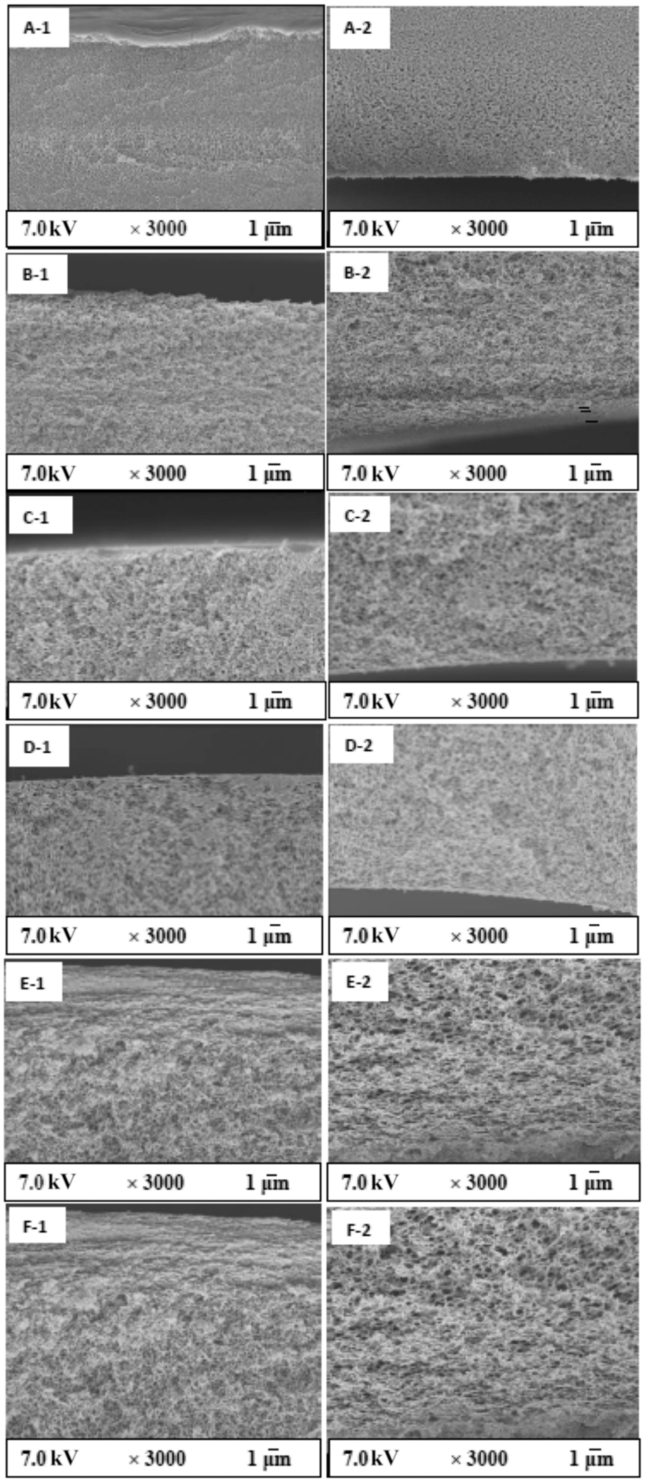

Figure 5. Cross-sectional SEM images of prepared hollow fiber membranes. (1) Near the outer surface, (2) near the inner surface. Labels in the top left corner identify the polymer solution and the air gap (for detailed information, see Table 2).

(several hundred nanometers). These results confirm our claim that the air gap has a dominant effect on forming the outer surface because the only difference of B vs D and A vs C is the air gap distance.

According to Figure 6, the inner surfaces of the prepared membranes are entirely porous with a large pore size, which are the typical inner surface structures of TIPS membranes (A-

https://doi.org/10.1021/acsomega.2c01773
ACS Omega 2022, 7, 33783−33792

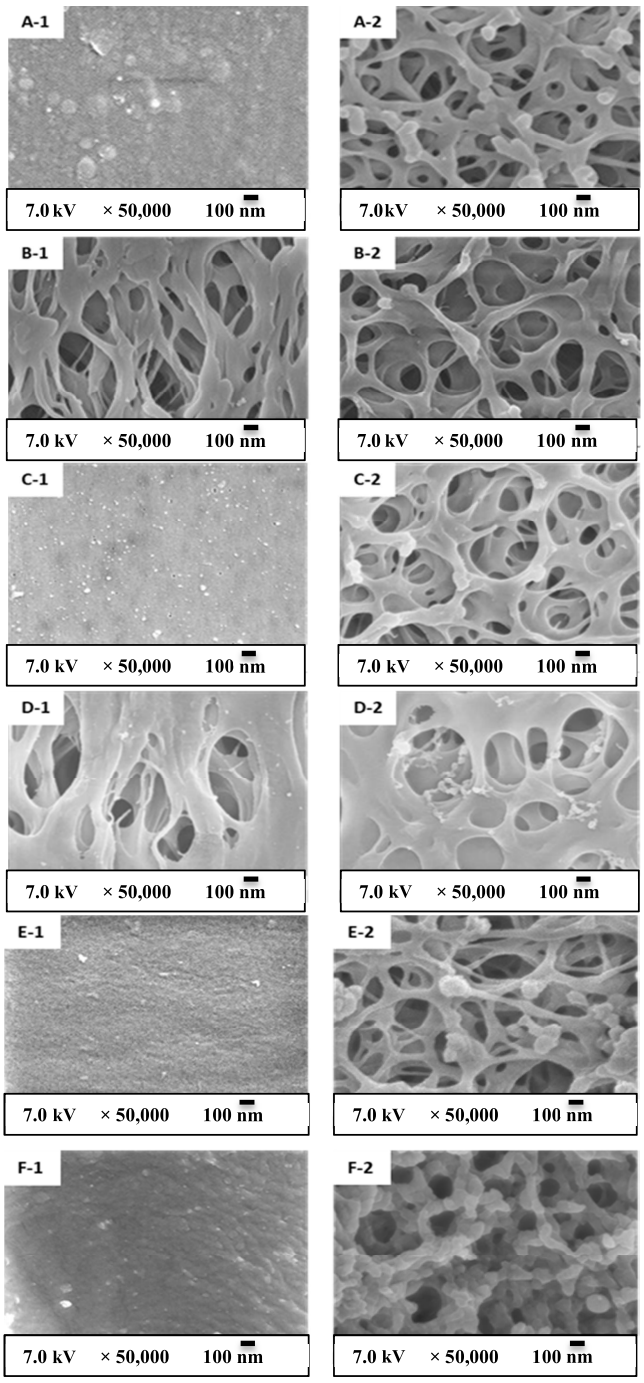

Figure 6. Surface SEM images of the prepared hollow fiber membranes. (1) Outer surface, (2) inner surface. Labels in the top left corner identify the polymer solution and the air gap (for detailed information, see Table 2).

2−F-2).[21,37] No solvent evaporation occurred on the inner surface because the polymer solution there was in contact with the bore liquid. This results in a porous structure. In the cases of CTA/SF/NPG and CTA/SF/1,3-BG with an air gap distance of 0 mm, the pore sizes on the inner surface (Figure 6B-2,D-2) were slightly larger than those at the outer surface (Figure 6B-1,D-1). The cooling rate at the inner surface was also lower because the polymer solution was in contact with the hot bore liquid there. The lower cooling rate is probably the reason for the larger pore size.

3.3.2. Pure Water Permeance (PWP) and Particle Rejection. Table 3 shows the PWP values of hollow fiber membranes prepared with different cellulose derivatives. When the air gap distance was 5 mm, the PWP values were considerably low. Except for the CDA/EHD membrane (membrane E) with a PWP of 102 L/(m^2·h·bar), all other membranes had PWP <30 L/(m^2·h·bar). These data are entirely in line with the SEM images in Figure 6, which show a dense or very low porosity outer surface for membranes A, C, E, and F. In contrast, the CTA membranes had much higher PWP: 610 L/(m^2·h·bar) for membrane B and 952 L/(m^2·h·bar) for membrane D. Considering the SEM images of these two membranes (Figures 5 and 6) and their PWP results (Table 3), we conclude that the MF-type hollow fiber membranes were prepared successfully.

Table 3. Pure Water Permeance (PWP) of Hollow Fiber Membranes Prepared from Cellulose Derivatives

membrane code	air gap (mm)	PWP [L/(m^2 h bar)]
A: CTA/SF/NPG	5	28
B: CTA/SF/NPG	0	610
C: CTA/SF/1,3-BG	5	30
D: CTA/SF/1,3-BG	0	952
E: CDA/EHD	5	102
F: CAP/EHD	5	7

The rejection properties of membrane D, which had the highest water permeance, were evaluated using 100 nm silica nanoparticles (Table 4). This membrane rejected 99% of the nanoparticles according to Table S6. To the best of our knowledge, this is the first report of CTA hollow fiber membranes prepared with a binary solvent that exhibited acceptable PWP and notable rejection of 100 nm silica nanoparticles.

Table 4. Rejection of the Prepared CTA Membrane with the Highest Water Permeability

sample	pure water permeance [L/(m^2 h bar)]	rejection of 100 nm silica particle [%]
D	952	99

These results show that this study's CTA prepared hollow fiber membranes to show a considerable advantage over other CA derivatives membranes. As shown in Table S6, while the elongation of the different CA derivatives prepared membranes is almost comparable, the maximum stress at break of the CTA was 3−5 times higher than that of the CDA and CAP. Thus, we think our effort to screen for suitable solvents for CTA was successful.

Considering the CTA material properties, higher antifouling, and better anti-biodegradation properties as mentioned in the Introduction section, it is expected that prepared MF membrane can be appropriately applied in pharmaceutical industries.

4. CONCLUSIONS

Based on our previous knowledge and expertise, in this study, we prepared CTA MF hollow fiber membranes via the thermally induced phase separation (TIPS) method and compared the results with those of CDA and CAP hollow fiber membranes. Extensive solvent screening was performed

https://doi.org/10.1021/acsomega.2c01773
ACS Omega 2022, 7, 33783−33792

to identify suitable solvent systems. The three polymers CTA, CDA, and CAP showed different phase separation mechanisms in solutions. Two ternary mixtures of CTA and two organic solvents (CTA/SF/NPG and CTA/SF/1,3-BG) were suitable for membrane preparation with liquid−liquid phase separation followed by polymer crystallization. All of the prepared membranes showed a completely interconnected structure, with ca. 100 nm pores in the membrane bulk structure and a porous inner surface. In contrast, the outer surface structure depended on the air gap distance: a porous structure was formed at an air gap distance of 0 mm, while a dense structure was formed at 5 mm. When using a 0 mm air gap distance, a suitable binary solvent system, and a solvent for cellulose derivatives as the quench bath medium, it was possible to obtain a CTA MF hollow fiber membrane with a PWP of ∼1000 L/(m2 h bar) and almost complete rejection of 100 nm silica nanoparticles. The prepared CTA membranes showed maximum stress at break 3−5 times higher than those of the CDA and CAP. This is the first report of MF CTA hollow fiber membranes with acceptable PWP and a high particle rejection rate. The produced CTA MF hollow fiber membrane has gear potential to be used in pharmaceutical applications.

■ ASSOCIATED CONTENT

Supporting Information

The Supporting Information is available free of charge at https://pubs.acs.org/doi/10.1021/acsomega.2c01773.

Hansen solubility parameter (HSP) and melting temperature of cellulose derivatives polymers and solvents used in the solvent screening; number of solvents dissolved polymer at 170 °C and R_a of the cellulose derivative with the evaluated solvents; number of appropriate solvents for TIPS process and R_a of the cellulose derivative with the evaluated solvents; HSP of cellulose derivatives polymers and selected solvents used in the membrane preparation; R_a of cellulose derivatives polymers and selected solvents used in the membrane preparation; relationship between SF/NPG ratio and CTA/SF/NPG polymer solution state; and mechanical strength and stretch of the prepared hollow fiber membrane from the cellulose derivative (Tables S1−S7) (PDF)

■ AUTHOR INFORMATION

Corresponding Author

Tomohisa Yoshioka − *Graduate School of Science, Technology and Innovation, Kobe University, Kobe 657-8501, Japan; Research Center for Membrane and Film Technology, Kobe University, Kobe 657-8501, Japan;* orcid.org/0000-0002-7489-441X; Email: tom@opal.kobe-u.ac.jp

Authors

Shota Takao − *Daicel Co., Ltd., Himeji 671-1283, Japan; Graduate School of Science, Technology and Innovation, Kobe University, Kobe 657-8501, Japan*

Saeid Rajabzadeh − *Research Center for Membrane and Film Technology and Department of Chemical Science and Engineering, Kobe University, Kobe 657-8501, Japan;* orcid.org/0000-0003-2883-4587

Chihiro Otsubo − *Daicel Co., Ltd., Himeji 671-1283, Japan*

Toyozo Hamada − *Daicel Co., Ltd., Himeji 671-1283, Japan*

Noriaki Kato − *Graduate School of Science, Technology and Innovation, Kobe University, Kobe 657-8501, Japan; Research Center for Membrane and Film Technology and Department of Chemical Science and Engineering, Kobe University, Kobe 657-8501, Japan*

Keizo Nakagawa − *Graduate School of Science, Technology and Innovation, Kobe University, Kobe 657-8501, Japan; Research Center for Membrane and Film Technology, Kobe University, Kobe 657-8501, Japan;* orcid.org/0000-0002-5323-0462

Takuji Shintani − *Graduate School of Science, Technology and Innovation, Kobe University, Kobe 657-8501, Japan; Research Center for Membrane and Film Technology, Kobe University, Kobe 657-8501, Japan*

Hideto Matsuyama − *Research Center for Membrane and Film Technology and Department of Chemical Science and Engineering, Kobe University, Kobe 657-8501, Japan;* orcid.org/0000-0003-2468-4905

Complete contact information is available at: https://pubs.acs.org/10.1021/acsomega.2c01773

Notes

The authors declare no competing financial interest.

■ REFERENCES

(1) Mulder, M. *Basic Principles of Membrane Technology*, Kluwer Academic Publisher, 1997; p 576.

(2) Mollahosseini, A.; Abdelrasoul, A.; Shoker, A. A Critical Review of Recent Advances in Hemodialysis Membranes Hemocompatibility and Guidelines for Future Development. *Mater. Chem. Phys.* **2020**, *248*, No. 122911.

(3) Budtova, T.; Navard, P. Cellulose in NaOH−Water Based Solvents: A Review. *Cellulose* **2016**, *23*, 5−55.

(4) Wang, D. A Critical Review of Cellulose-Based Nanomaterials for Water Purification in Industrial Processes. *Cellulose* **2019**, *26*, 687−701.

(5) Douglass, E. F.; Avci, H.; Boy, R.; Rojas, O. J.; Kotek, R. A Review of Cellulose and Cellulose Blends for Preparation of Bio-Derived and Conventional Membranes, Nanostructured Thin Films, and Composites. *Polym. Rev.* **2018**, *58*, 102−163.

(6) Ho, N. A. D.; Leo, C. P. A Review on the Emerging Applications of Cellulose, Cellulose Derivatives and Nanocellulose in Carbon Capture. *Environ. Res.* **2021**, *197*, No. 111100.

(7) Lu, P.; Gao, Y.; Umar, A.; Zhou, T.; Wang, J.; Zhang, Z.; Huang, L.; Wang, Q. Recent Advances in Cellulose-Based Forward Osmosis Membrane. *Sci. Adv. Mater.* **2015**, *7*, 2182−2192.

(8) Sjahro, N.; Yunus, R.; Abdullah, L. C.; Rashid, S. A.; Asis, A. J.; Akhlisah, Z. N. Recent Advances in the Application of Cellulose Derivatives for Removal of Contaminants from Aquatic Environments. *Cellulose* **2021**, *28*, 7521−7557.

(9) Doelker, E. *Cellulose Derivatives*; Springer: Berlin, 1993; pp 199−265.

(10) Laîné, J.-M.; Campos, C.; Baudin, I.; Janex, M.-L. Understanding Membrane Fouling: A Review of Over a Decade of Research. *Water Supply* **2003**, *3*, 155−164.

(11) Yu, Y.; Wu, Q.-Y.; Liang, H.-Q.; Gu, L.; Xu, Z.-K. Preparation and Characterization of Cellulose Triacetate Membranes via Thermally Induced Phase Separation. *J. Appl. Polym. Sci.* **2017**, *134*, 44454.

(12) Koseoglu-Imer, D. Y.; Dizge, N.; Koyuncu, I. Enzymatic Activation of Cellulose Acetate Membrane for Reducing of Protein Fouling. *Colloids Surf., B* **2012**, *92*, 334−339.

(13) Ul-Islam, M.; Ul-Islam, S.; Yasir, S.; Fatima, A.; Ahmed, W. M.; Lee, S. Y.; Manan, S.; Ullah, W. M. Potential Applications of Bacterial Cellulose in Environmental and Pharmaceutical Sectors. *Curr. Pharm. Des.* **2020**, *26*, 5793−5806.

https://doi.org/10.1021/acsomega.2c01773
ACS Omega 2022, 7, 33783−33792

(14) Higuchi, A.; Tamai, M.; Ko, Y.-A.; Tagawa, Y.-I.; Wu, Y.-H.; Freeman, B. D.; Bing, J.-T.; Chang, Y.; Ling, Q.-D. Polymeric Membranes for Chiral Separation of Pharmaceuticals and Chemicals. *Polym. Rev.* **2010**, *50*, 113−143.
(15) Sakai, K.; Yamauchi, T.; Nakasu, F.; Ohe, T. Biodegradation of Cellulose Acetate by Neisseria sicca. *Biosci. Biotechnol. Biochem.* **1996**, *60*, 1617−1622.
(16) Ghaffarian, V.; Mousavi, S. M.; Bahreini, M.; Shoaei Parchin, N. Biodegradation of Cellulose Acetate/Poly(butylene succinate) Membrane. *Int. J. Environ. Sci. Technol.* **2017**, *14*, 1197−1208.
(17) Luo, W.; Xie, M.; Hai, F. I.; Price, W. E.; Nghiem, L. D. Biodegradation of Cellulose Triacetate and Polyamide Forward Osmosis Membranes in an Activated Sludge Bioreactor: Observations and Implications. *J. Membr. Sci.* **2016**, *510*, 284−292.
(18) Lloyd, D. R.; Kinzer, K. E.; Tseng, H. S. Microporous Membrane Formation via Thermally Induced Phase Separation. I. Solid-Liquid Phase Separation. *J. Membr. Sci.* **1990**, *52*, 239−261.
(19) Ren, J.; Wang, R. Preparation of Polymeric Membranes. In *Membrane and Desalination Technologies*, Wang, L. K.; Chen, J. P.; Hung, Y.-T.; Shammas, N. K., Eds.; Humana Press, 2008; Vol. *13*, pp 47−100.
(20) Matsuyama, H.; Karkhanechi, H.; Rajabzadeh, S. Polymeric Membrane Fabrication via Thermally Induced Phase Separation (TIPS) Method. In *Hollow Fiber Membranes*, Chung, T.-S.; Feng, Y., Eds.; Elsevier, 2021; Chapter 3, pp 57−83.
(21) Shibutani, T.; Kitaura, T.; Ohmukai, Y.; Maruyama, T.; Nakatsuka, S.; Watabe, T.; Matsuyama, H. Membrane Fouling Properties of Hollow Fiber Membranes Prepared from Cellulose Acetate Derivatives. *J. Membr. Sci.* **2011**, *376*, 102−109.
(22) Fu, X. Y.; Sotani, T.; Matsuyama, H. Effect of Membrane Preparation Method on the Outer Surface Roughness of Cellulose Acetate Butyrate Hollow Fiber Membrane. *Desalination* **2008**, *233*, 10−18.
(23) Xing, X.-Y.; Gu, L.; Jin, Y.; Sun, R.; Xie, M.-Y.; Wu, Q.-Y. Fabrication and Characterization of Cellulose Triacetate Porous Membranes by Combined Nonsolvent-Thermally Induced Phase Separation. *Cellulose* **2019**, *26*, 3747−3762.
(24) Hansen, C. M. *Hansen Solubility Parameters: A User's Handbook*, 2nd ed.; CRC Press, 2007.
(25) Fang, C.; Jeon, S.; Rajabzadeh, S.; Cheng, L.; Fang, L.; Matsuyama, H. Tailoring the surface pore size of hollow fiber membranes in the TIPS process. *J. Mater. Chem. A* **2018**, *6*, 20712−20724.
(26) Fang, C.; Jeon, S.; Rajabzadeh, S.; Fang, L.-F.; Cheng, L.; Matsuyama, H. Tailoring both the surface pore size and sub-layer structures of PVDF membranes prepared by the TIPS process with a triple orifice spinneret. *J. Mater. Chem. A* **2018**, *6*, 20712−20724.
(27) Kim, K.; Ingole, P. G.; Kim, J.-H.; Lee, H.-K. Separation performance of PEBAX/PEI hollow fiber composite membrane for $SO_2/CO_2/N_2$ mixed gas. *Chem. Eng. J.* **2013**, *233*, 242−250.
(28) Choi, W.; Ingole, P. G.; Parka, J.-S.; Lee, D.-W.; Kim, J.-H.; Lee, H.-K. H_2/CO mixture gas separation using compositehollow fiber membranes prepared by interfacialpolymerization method. *Chem. Eng. Res. Des.* **2015**, *102*, 297−306.
(29) Choi, W.; Ingole, P. G.; Li, H.; Kim, J.-H.; Lee, H.-K.; Baek, I.-H. Preparation of facilitated transport hollow fiber membrane for gas separation using cobalt tetraphenylporphyrin complex as a coating material. *J. Cleaner Prod.* **2016**, *133*, 1008−1016.
(30) Rajabzadeh, S.; Maruyama, T.; Sotani, T.; Matsuyama, H. Preparation of PVDF hollow fiber membrane from a ternary polymer/solvent/non-solvent system via thermally induced phase separation (TIPS) method. *Sep. Purif. Technol.* **2008**, *63*, 415−423.
(31) Shang, M.; Matsuyama, H.; Teramoto, M.; Lloyd, D. R.; Kubota, N. Preparation and Membrane Performance of Poly(ethylene-co-vinyl alcohol) Hollow Fiber Membrane via Thermally Induced Phase Separation. *Polymer* **2003**, *44*, 7441−7447.
(32) Matsuyama, H.; Ohga, K.; Maki, T.; Tearamoto, M.; Nakatsuka, S. Porous Cellulose Acetate Membrane Prepared by Thermally Induced Phase Separation. *J. Appl. Polym. Sci.* **2003**, *89*, 3951−3955.
(33) Nguyen, T. P. N.; Yun, E.-T.; Kim, I.-C.; Kwon, Y.-N. Preparation of Cellulose Triacetate/Cellulose Acetate (CTA/CA)-Based Membranes for Forward Osmosis. *J. Membr. Sci.* **2013**, *433*, 49−59.
(34) Li, H.-J.; Cao, Y.-M.; Qin, J.-J.; Jie, X.-M.; Wang, T.-H.; Liu, J.-H.; Yuan, Q. Development and Characterization of Anti-Fouling Cellulose Hollow Fiber UF Membranes for Oil−Water Separation. *J. Membr. Sci.* **2006**, *279*, 328−335.
(35) Matsuyama, H.; Yuasa, M.; Kitamura, Y.; Teramoto, M.; Lloyd, D. R. Structure Control of Anisotropic and Asymmetric Polypropylene Membrane Prepared by Thermally Induced Phase Separation. *J. Membr. Sci.* **2000**, *179*, 91−100.
(36) Matsuyama, H.; Rajabzadeh, S.; Karkhanechi, H.; Jeon, S. PVDF Hollow Fibers Membranes. In *Comprehensive Membrane Science and Engineering*, Elsevier Science, 2017; pp 137−189.
(37) Liu, Y.; Liu, Z.; Morisato, A.; Bhuwania, N.; Chinn, D.; Koros, W. J. Natural Gas Sweetening Using a Cellulose Triacetate Hollow Fiber Membrane Illustrating Controlled Plasticization Benefits. *J. Membr. Sci.* **2020**, *601*, No. 117910.
(38) Raza, A.; Farrukh, S.; Hussain, A.; Khan, I.; Othman, M. H. D.; Ahsan, M. Performance Analysis of Blended Membranes of Cellulose Acetate with Variable Degree of Acetylation for CO_2/CH_4 Separation. *Membranes* **2021**, *11*, 245.
(39) Rajabzadeh, S.; Maruyama, T.; Sotani, T.; Matsuyama, H. Preparation of PVDF Hollow Fiber Membrane from a Ternary Polymer/Solvent/Nonsolvent System via Thermally Induced Phase Separation (TIPS) Method. *Sep. Purif. Technol.* **2008**, *63*, 415−423.

https://doi.org/10.1021/acsomega.2c01773
ACS Omega 2022, 7, 33783−33792